

# Dithiolate-Appended Iridium(III) Complex with Dual Functions of Reducing and Capping Agent for the Design of Small-Sized Gold Nanoparticles

Gihane Nasr,<sup>†</sup> Audrey Guerlin,<sup>†,‡</sup> Frédéric Dumur,<sup>§</sup> Stéphane A. Baudron,<sup>||</sup> Eddy Dumas,<sup>†</sup> Fabien Miomandre,<sup>‡</sup> Gilles Clavier,<sup>‡</sup> Michel Sliwa,<sup>⊥</sup> and Cédric R. Mayer<sup>\*,†</sup>

<sup>†</sup>Institut Lavoisier de Versailles, Université de Versailles Saint-Quentin en Yvelines, UMR 8180 CNRS, 78035 Versailles, France

<sup>‡</sup>Institut d'Alembert, IFR 121, Ecole Normale Supérieure de Cachan, 94235 Cachan, France

<sup>§</sup>Laboratoire Chimie Provence, équipe CROPS, UMR 6264 CNRS, Universités d'Aix-Marseille I, II, III, 13397 Marseille, France

<sup>||</sup>Laboratoire de Chimie de Coordination Organique, Université de Strasbourg, UMR 7140 CNRS, 67000 Strasbourg, France

<sup>⊥</sup>Laboratoire de Spectrochimie Infrarouge et Raman, UMR-CNRS 8516, Université Lille Nord de France, Université Lille 1 Sciences et Technologies de Lille, 59655 Villeneuve d'Ascq, France

 Supporting Information

**ABSTRACT:** The unprecedented combined reduction of chloroauric acid and capping of the resulting gold nanoparticles in the absence of an external reducing agent are demonstrated using a novel heteroleptic Ir(III) complex incorporating a 4,5-diazafluorenedithiolate ligand. The reduction process in basic medium results from a cascade mechanism involving oxidation of the ligand, reduction of the gold salt, and stabilization and functionalization of the gold nanoparticles.

Over the past few years, complexes of heavy transition metals [Ru(II), Os(II), etc.], with an emphasis on polypyridyl species, have been the focus of numerous studies because of their unique photophysical and photochemical properties as well as their attractive long-lived excited states.<sup>1–4</sup> Neutral and charged Ir(III) complexes, which exhibit phosphorescence efficiencies close to unity,<sup>5</sup> have especially attracted a great deal of interest in organic light-emitting diodes (OLEDs)<sup>6–10</sup> or light-emitting electrochemical cells (LECs).<sup>11,12</sup> The variability of their electro-optical properties has also promoted their application in light-to-energy conversion and sensors and as efficient catalysts for arylation of olefins or hydrogenation.<sup>13</sup> In parallel, gold nanoparticles (AuNPs) have been the object of intense research efforts<sup>14</sup> driven by their widespread applications ranging from catalysis for small-sized particles<sup>15</sup> to optoelectronics<sup>16</sup> and biomedical materials.<sup>17</sup> Interestingly, the functionalization of AuNPs by polypyridyl Ir(III) complexes has to our knowledge not been reported. The design of complex-capped gold nanocomposites requires care because the byproducts generated by reducing agents cause damage in the targeted applications of the nanocomposites, notably in biosystems and optoelectronics. Several synthetic approaches have been proposed, such as direct functionalization, postfunctionalization by a complex, and use of a proligand followed by its complexation.<sup>18</sup> Heteroditopic bidentate 4,5-diaza-9-[4,5-bis(2-cyanoethylsulfanyl)-1,3-dithiol-2-ylidene]fluorene [FluoDT(SPN)<sub>2</sub>]

proligands are appealing candidates to serve as the bridging ligands between the NPs and the complexes. Upon deprotection of the thiol functions, these molecules feature two chelates, a dianionic sulfur-based one and a neutral nitrogen-based one, allowing the preparation of novel homo/heterometallic infinite architectures.<sup>19–21</sup> To the best of our knowledge, the corresponding dithiolates have never been used as a dual linker capable of bridging cationic metallic complexes and metallic NPs.

Herein we report the heteroleptic Ir(III) complex [Ir(dfppy)<sub>2</sub>(FluoDT(SPN)<sub>2</sub>)]<sup>+</sup> (**1**) [dfppy = 2-(2,4-difluorophenyl)pyridine], which features a 4,5-diazafluorenedithiolate ligand that is capable of acting as both an efficient reductant for tetrachloroauric acid and a capping agent of AuNPs in a cascade mechanism. We have investigated this process using UV–vis spectroscopy, density functional theory (DFT) calculations, and cyclic voltammetry.

The cationic Ir(III) complex **1** was prepared in a one-step synthesis by complexation of FluoDT(SPN)<sub>2</sub> with the cyclometalated Ir(III) di-*μ*-chloro-bridged dimer [(dfppy)<sub>2</sub>IrCl]<sub>2</sub> in 50% yield. Next, for preparation of monodisperse and stable colloidal suspensions, the thiolate groups could only ensure strong binding of the complex to the AuNPs after removal of the propionitrile (PN) protecting groups on **1**. Interestingly, upon deprotection of the thiols under basic conditions in CH<sub>3</sub>CN, spontaneous reduction of HAuCl<sub>4</sub> occurred, forming a colloidal suspension with an average particle diameter of 2–3 nm, as confirmed by TEM and DLS (Figure 1). In solvents with various polarities, the reduction phenomenon occurred in solvents such as H<sub>2</sub>O, MeOH, dichloromethane (DCM), and CH<sub>3</sub>CN, with a faster reduction process observed in the latter. Studies of the uncomplexed deprotected ligand FluoDT(S<sup>−</sup>)<sub>2</sub> demonstrated that only a very slow reduction process could be observed only in CH<sub>3</sub>CN. These experimental results clearly proved the essential role of the metallic Ir(III) center in the reduction process. However, significant differences in the stability of the resulting Au<sup>0</sup>–**1** nanocomposites were observed, with flocculation in solvents such as CH<sub>3</sub>CN or MeOH. However, this unexpected flocculation was

Received: December 17, 2010

Published: April 08, 2011

extremely advantageous, as it provided a facile purification method for the separation of the nanocomposites from the excess ungrafted complexes. After purification by centrifugation, the flocculated NPs were dispersed in *N,N*-dimethylformamide (DMF), and the particles proved to be highly stable over time. Therefore, all further spectroscopic investigations were performed in this solvent. For the rest of the study, the nanocomposites were synthesized in MeOH and dispersed in DMF after purification by centrifugation.

To highlight the unique design of the reducing/capping agent, further investigations were carried out with the protected complex **1** and the model complex  $[\text{Ir}(\text{dfppy})_2(\text{bpy})]^+$  ( $\text{bpy} = 2,2'$ -bipyridine). In all cases, no reduction of  $\text{HAuCl}_4$  was observed, thus indicating that the reducing characters of the two Ir(III) complexes were not sufficient to reduce  $\text{HAuCl}_4$  into AuNPs without the help of an additional reducing agent. When the  $\text{FluoDT}(\text{S}^-)_2$  ligand was used as a reducing and capping agent for AuNPs in a direct functionalization strategy in  $\text{CH}_3\text{CN}$ , an AuNP nanocomposite with a particle size of 3–4 nm, similar to that of  $\text{Au}^0\text{-1}$ , was obtained. Postfunctionalization of this nanocomposite by complexation with  $[(\text{dfppy})_2\text{IrCl}]_2$  provided the targeted nanocomposite  $\text{Au}^0\text{-1}$ . The similarity in the size distributions for the nanocomposites obtained by direct functionalization or generation of a complex onto ligand-capped AuNPs in  $\text{CH}_3\text{CN}$  clearly demonstrates the strong binding affinity of the dithiolate groups for gold surfaces, thus preventing crystal growth of AuNPs and undesired desorption of the complex from the surface. Nevertheless, this strategy of post-functionalization by complexation on AuNPs is less advantageous because no aggregation occurred after complexation, making it difficult to purify the final nanocomposites from uncomplexed Ir(III) cations.

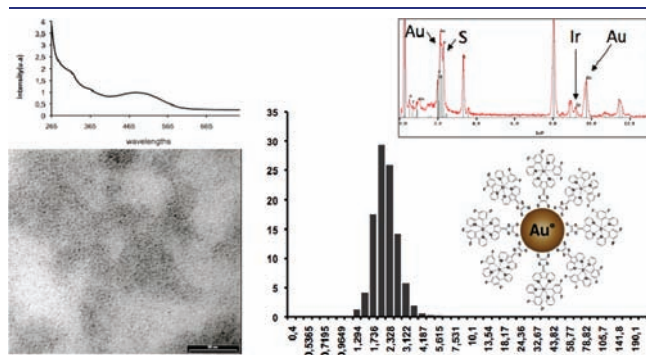


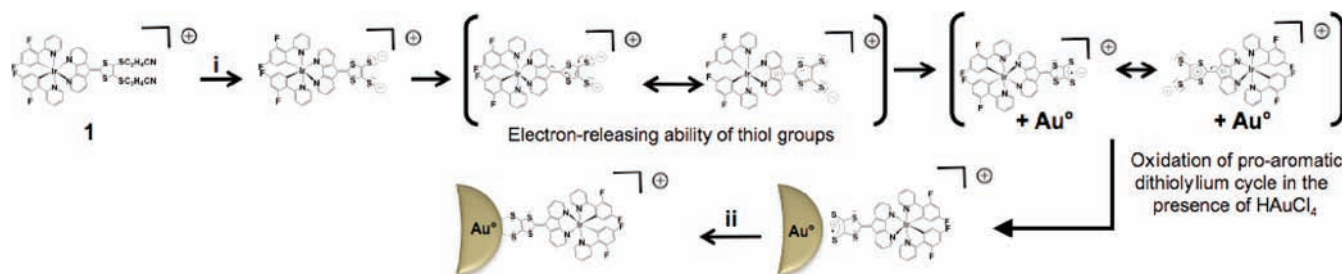
**Figure 1.** Analyses of  $\text{Au}^0\text{-1}$  nanocomposites obtained directly by deprotection of **1** in the presence of  $\text{HAuCl}_4$  under basic conditions: UV-vis spectrum, TEM image, EDX analysis, and DLS size distribution.

As a consequence, all the above-mentioned experiments clearly demonstrated the reducing character of the deprotected ligand when free or chelated to the Ir(III) complex. In particular, in the latter case, both the thiolate groups and the coordination of the diazafluorene site of the  $\text{FluoDT}(\text{S}^-)_2$  proligand to the Ir(III) complex moiety appeared to be essential to the promotion of a fast reduction process. Therefore, a mechanism illustrating the dual function of the final dithiolate complex could be deduced, as outlined in Scheme 1. When deprotected, thiols generate two electron-releasing groups, inducing a mesomeric form stabilized by the electron-withdrawing ability of the metal complex. Electron-donating dithiolate and diazafluorene anions enforce the oxidation of the proaromatic 1,3-dithiol-2-ylidene cycle by a mesomeric effect. Oxidation of the seven-electron cycle liberates one electron that is then used for the reduction of the gold salt, and the resulting 1,3-dithiolium-2-ylidene cycle is stabilized by aromaticity. In the meantime, the free radical is stabilized by its delocalization on the thiolate groups, and the strong binding affinity of thiolates for AuNPs both stabilizes the colloidal solution and limits the crystal growth of the particles. Finally, the neutrality of the ligand is regenerated by oxidation of one gold atom at the surface of the NP or by free radicals from the reaction medium, the reduction process being certainly activated by the presence of AuNPs. While Curtin et al.<sup>22</sup> recently reported the photoactivity of different Ir(III) complexes, it should be stressed that our synthesis of AuNPs was done in the dark to prevent any photodriven process that could happen during the reduction and capping process.

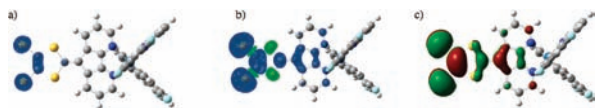
Herein the cationic Ir(III) center proved to be essential for accelerating the reduction process and stabilizing the resulting nanocomposite. In order to confirm this final hypothesis of reduction by the medium, a series of complementary experiments, DFT calculations, and  $^1\text{H}$  NMR analyses were carried out.  $^1\text{H}$  NMR spectra of the nanocomposites generated by post- and direct functionalization were recorded in  $\text{DMF-}d_7$  and confirmed the absence of radicals on the capping agent by their similarity to the spectrum obtained for the initial complex  $[\text{Ir}(\text{dfppy})_2(\text{FluoDT}(\text{SPN})_2)]\text{PF}_6$  and by the possibility of obtaining well-resolved NMR spectra of NP-bound complexes, even if significant line broadening, weaker signals, and higher relaxation rates were observed for the nanocomposites as a result of the small amount of Ir complexes on the AuNPs.<sup>23</sup>

DFT calculations also confirmed the proposed mechanism with the presence of the radical anion delocalized onto both dithiolate groups. Quantum-chemical calculations were carried out on the cationic, anionic, and radical Ir(III) complex  $[\text{Ir}(\text{dfppy})_2(\text{FluoDT}(\text{SPN})_2)]^+$ . DFT and time-dependent DFT (TD-DFT) calculations at the B3LYP level using a mixed basis set were performed [see the Supporting Information (SI) for details].

### Scheme 1. Mechanism of the Reduction and Capping Process: (i) Deprotection in a Basic Medium; (ii) Reduction by the Reaction Medium



**Scheme 2. Electron and Spin Densities from B3LYP Calculations for Radical Anions:** (a) Isodensity at 0.0004 au; (b) Isodensity at 0.004 au; (c) HSOMO Orbital



When calculations were performed on the radical complex, the unpaired electron was found to be mainly delocalized on the thiolate groups of the ligand (Scheme 2), in agreement with the proposed mechanism. A modification of the exocyclic S–C bond length was also observed, with the smallest S–C bonds obtained for the radical species. Thus, S–C bond lengths of 1.73, 1.71, and 1.82 Å were obtained for the anionic, radical, and cationic complexes, respectively, therefore supporting a more pronounced double-bond character of those bonds in the dianionic and monoanionic states, as proposed in the reaction mechanism.

The redox properties of the protected **1** and unprotected  $[\text{Ir}(\text{dfppy})_2(\text{FluoDT}(\text{S}^-)_2)]^+$  complexes were investigated by cyclic voltammetry. Figure SI14 shows that the latter can be oxidized at much lower potentials than the former, which is consistent with the HOMO being localized mainly on the  $[\text{Ir}(\text{dfppy})_2]^+$  or thiolate functions, respectively. The unprotected complex exhibits two successive oxidation steps associated with the formation of the radical anion and neutral forms on the fluorene-dithione part. The Ir(III)  $\rightarrow$  Ir(IV) conversion is shifted outside of the potential window for this complex in comparison with the parent protected one. The same behavior is observed for the  $\text{FluoDT}(\text{S}^-)_2$  and  $\text{FluoDT}(\text{SPN})_2$  proligands, with oxidation potentials in the same range. Thus, both of the unprotected moieties  $[\text{Ir}(\text{dfppy})_2(\text{FluoDT}(\text{S}^-)_2)]^+$  and  $\text{FluoDT}(\text{S}^-)_2$  can effect reduction of  $\text{HAuCl}_4$ , albeit with different kinetics according to the medium. The electrochemical results are supported by DFT calculations (see the SI). The HOMO is a contribution of Ir  $d_{xy}$  orbitals ( $t_{2g}$ ) and  $\pi$  orbitals of the two dfppy ligands. In contrast, the LUMO is mainly localized on the  $\text{FluoDT}(\text{SPN})_2$  unit.

The nanocomposites and the protected complexes were also characterized by UV–vis absorption spectroscopy. The electronic absorption spectrum of complex **1** in MeOH exhibited an intense broad band in the visible region with an absorption maximum centered at 456 nm ( $\epsilon = 18 \times 10^3 \text{ M}^{-1} \text{ cm}^{-1}$ ) and three other moderately intense UV–vis bands centered at 265 nm ( $\epsilon = 32.3 \times 10^3 \text{ M}^{-1} \text{ cm}^{-1}$ ), 296 nm ( $\epsilon = 23.8 \times 10^3 \text{ M}^{-1} \text{ cm}^{-1}$ ), and 321 nm ( $\epsilon = 15 \times 10^3 \text{ M}^{-1} \text{ cm}^{-1}$ ). With reference to previous work on Ir complexes,<sup>24</sup> the absorption bands at 250–350 nm were assigned to spin-allowed intraligand ( $\pi-\pi^*$ ) transitions and the visible absorption band detected at 456 nm to a mixture of the  $^1\text{LC}$  band of the  $\text{FluoDT}(\text{SPN})_2$  ligand and the Ir(III)  $\rightarrow$   $\text{FluoDT}(\text{SPN})_2$   $^1\text{MLCT}$  band, as further corroborated by TD-DFT calculations. The transitions calculated at 455, 425, and 397 nm originate from the HOMO  $\rightarrow$  LUMO, HOMO–1  $\rightarrow$  LUMO, and HOMO  $\rightarrow$  LUMO+1 transitions, respectively. These absorption bands are attributed to a mixed metal-to-ligand charge transfer (MLCT) and ligand(dfppy)–ligand(dithione) charge transfer (LLCT), as suggested by the compositions of the calculated frontier orbitals. Analogous to the LUMO, the HOMO–2 distribution primarily resides on the  $\text{FluoDT}(\text{SPN})_2$  unit. Consequently, the absorption at 406 nm, due to the HOMO–2( $\text{DT}(\text{SPN})_2$ )  $\rightarrow$  LUMO(Phen) transition,

suggests intraligand charge transfer (ILCT). The higher-energy transitions at 278 and 275 nm have a mixed ILCT/MLCT/LLCT character. The TD-DFT calculations showed some minor differences with experimental values because CT states are sensitive to solvent polarity and temperature, which were not included here.

The bathochromic shift of the visible band relative to that observed for free  $\text{FluoDT}(\text{SPN})_2$  ( $\lambda = 415 \text{ nm}$ ,  $\epsilon = 13.3 \times 10^3 \text{ M}^{-1} \text{ cm}^{-1}$ ) was ascribed to the coordination of the ligand to the metal cation.<sup>25</sup> This shift was markedly observed when Ir was used as the metal, and such an intense visible band has rarely been reported in the literature for cationic Ir complexes.<sup>26</sup> When the dithiol functions were deprotected, the visible band at 456 nm was strongly red-shifted to 509 nm ( $\epsilon = 11.6 \times 10^3 \text{ M}^{-1} \text{ cm}^{-1}$ ). Similarly, bathochromic shifts of the UV–vis bands were also observed (from 296 to 318 and 321 to 359 nm, respectively). The shifts of both the UV and visible bands were assigned to the electron-releasing character of the dithiolate ligand, which stabilizes the electron-deficient complex. The reduction of the Au(III) salt by the complex was monitored in time by UV–vis absorption spectroscopy. After addition of the gold salt, a decrease in the Au(III) band (323 nm) and a hypsochromic shift of the visible band (ca. 474 nm, corresponding to the combination of the  $^1\text{LC}$  and  $^1\text{MLCT}$  bands) were observed in a first stage, followed in a second stage by the emergence of the surface plasmon band (SPB) of AuNPs at 493 nm and finally by the appearance of a long tail extending further toward lower energy and originating from the flocculation of the AuNPs. The UV–vis spectrum of the final nanocomposite in DMF showed a broad band centered at 495 nm combining at high energy a band with the typical signature of a colloidal suspension based on small-sized AuNPs with the characteristic feature band of the complex at low energy. The presence of a single monolayer composed of a limited number of Ir complexes at the surface of each AuNP explains the weak intensity of the band observed for the complex when grafted on NPs.

Luminescence characterizations were performed on nanocomposites in DMF and, for comparison, on **1**·PF<sub>6</sub> and the model complex  $[\text{Ir}(\text{dfppy})_2(\text{bpy})]\text{PF}_6$ . Whereas the nanocomposites in DMF showed no luminescence, upon photoexcitation at 390 nm in an oxygen-free CH<sub>3</sub>CN solution (same polarity as DMF), the luminescence profiles of **1** and the model complex displayed emission bands with maxima centered at 565 and 537 nm, respectively, attributed to a  $^3\pi-\pi^*$  transition with an admixture of  $^3\text{MLCT}$  character (Table 1 and Figures SI5 and SI6). This was confirmed by a strong quenching of the emission in the presence of oxygen (Figure SI7). The emission lifetimes were ca. 1.4  $\mu\text{s}$  and 440 ps for the model complex and **1**, respectively (Figures SI7 and SI8). Moreover, the quantum yield of the model complex was high (ca. 0.4), as reported for similar Ir(III) complexes,<sup>27a</sup> whereas for **1** it was a hundred times smaller, thus traducing an electron and/or energy transfer between the Ir(III) and dithiolene moieties.<sup>27b,c</sup> When **1** was grafted on AuNPs, an additional quenching effect due to the AuNPs was registered, similar to that for Ru complexes bound to AuNPs, and thus no luminescence was observed as a result of the close proximity of the complexes to the NPs.<sup>28</sup> Rationalization of the formation and deactivation pathway of the luminescent  $^3\text{MLCT}$  state using femtosecond transient absorption experiments is in progress (Figure SI8).

In conclusion, the first metallic complex exhibiting the dual function of reducing and capping agent has been reported. The



**Table 1. Emission  $\lambda_{\text{max}}$ , Quantum Yield, and Lifetime of the MLCT Triplet State for  $[\text{Ir}(\text{dfppy})_2(\text{bpy})]\text{PF}_6$  and  $1 \cdot \text{PF}_6$  in Degassed Acetonitrile and for Nanocomposites in DMF**

sample	$\lambda_{\text{max}}$ (nm)	quantum yield	lifetime
$[\text{Ir}(\text{dfppy})_2(\text{bpy})]\text{PF}_6$	537	0.4	1.4 $\mu\text{s}$
$1 \cdot \text{PF}_6$	565	0.003	440 ps
$\text{Au}^0-1$		no emission	

unique design of this Ir complex allowed the generation of AuNPs of extremely small sizes. Reduction of  $\text{HAuCl}_4$  by the complex was initiated under basic conditions by the deprotection of the two thiol functions, resulting in reduction of the gold salt and in situ functionalization of the resulting AuNPs by a cascade mechanism. The nanocomposites thus generated constitute promising candidates in catalysis [because of the unique combination of the strong activity of small-sized NPs with the well-reported properties of Ir(III) complexes], for electronic devices, and as a dye for solar cells.<sup>29</sup>

## ■ ASSOCIATED CONTENT

**S Supporting Information.** Experimental and theoretical procedures and results of characterizations and theoretical calculations. This material is available free of charge via the Internet at <http://pubs.acs.org>.

## ■ AUTHOR INFORMATION

**Corresponding Author**  
cmayer@chimie.uvsq.fr

## ■ ACKNOWLEDGMENT

We thank the ANR "JC–JC" in the frame of the AURUS Program (ANR-07-JCJC-040) and the CNRS for financial support. P. Beaunier (LRS, UMR-7197, UPMC) and C. Longin (INRA, UR-1196) are also acknowledged for their kind assistance with TEM and HRTEM images and EDX analysis.

## ■ REFERENCES

- (1) (a) Haas, K. L.; Franz, K. *Chem. Rev.* **2009**, *109*, 4921. (b) Perrier, S.; Mugeniwabagara, E.; Kirsch-De Mesmaeker, A.; Hore, P. J.; Luhmer, M. *J. Am. Chem. Soc.* **2009**, *131*, 12458. (c) Indelli, M. T.; Carli, S.; Ghirelli, M.; Chiorboli, C.; Ravaglia, M.; Garavelli, M.; Scandola, F. *J. Am. Chem. Soc.* **2008**, *130*, 7286.
- (2) DeClue, M. S.; Monnard, P.-A.; Bailey, J. A.; Maurer, S. E.; Collis, G. E.; Ziocck, H.-J.; Rasmussen, S.; Boncella, J. M. *J. Am. Chem. Soc.* **2009**, *131*, 931.
- (3) MacQueen, D. B.; Schanze, K. S. *J. Am. Chem. Soc.* **1991**, *113*, 6108.
- (4) (a) Nazeeruddin, M. K.; Klein, C.; Liska, P.; Grätzel, M. *Coord. Chem. Rev.* **2005**, *249*, 1460. (b) Polo, A. S.; Itokazu, M. K.; Frin, K. M.; de Patrocínio, A. O. T.; Murakami Iha, N. Y. *Coord. Chem. Rev.* **2006**, *250*, 1669.
- (5) Ulbricht, C.; Beyer, B.; Friebe, C.; Winter, A.; Schubert, U. S. *Adv. Mater.* **2009**, *21*, 4418.
- (6) (a) Baldo, M. A.; Lamansky, S.; Burrows, P. E.; Thompson, M. E.; Forrest, S. R. *Appl. Phys. Lett.* **1999**, *75*, 4. (b) Sajoto, T.; Djurovich, P. I.; Tamayo, A.; Yousufuddin, M.; Bau, R.; Thompson, M. E.; Holmes, R. J.; Forrest, S. R. *Inorg. Chem.* **2005**, *44*, 7992.
- (7) Hofbeck, T.; Yersin, H. *Inorg. Chem.* **2010**, *49*, 9290.
- (8) Nazeeruddin, M. K.; Humphry-Baker, R.; Berner, D.; Rivier, S.; Zuppiroli, L.; Grätzel, M. *J. Am. Chem. Soc.* **2003**, *125*, 8790.
- (9) Chang, C.-F.; Cheng, Y.-M.; Chi, Y.; Chiu, Y.-C.; Lin, C.-C.; Lee, G.-H.; Chou, P.-T.; Chen, C.-C.; Chang, C.-H.; Wu, C.-C. *Angew. Chem.* **2008**, *120*, 4618.
- (10) Baranoff, E.; Suarez, S.; Bugnon, P.; Barolo, C.; Buscaino, R.; Scopelliti, R.; Zuppiroli, L.; Grätzel, M.; Nazeeruddin, M. K. *Inorg. Chem.* **2008**, *47*, 6575.
- (11) (a) Slinker, J. D.; Gorodetsky, A. A.; Lowry, M. S.; Wang, J.; Parker, S.; Rohl, R.; Bernhard, S.; Malliaras, G. G. *J. Am. Chem. Soc.* **2004**, *126*, 2763. (b) Zysman-Colman, E.; Slinker, J. D.; Parker, J. B.; Malliaras, G. G.; Bernhard, S. *Chem. Mater.* **2008**, *20*, 388.
- (12) Mydiak, M.; Bizzami, C.; Hartmann, D.; Sarfert, W.; Schmid, G.; De Cola, L. *Adv. Funct. Mater.* **2010**, *20*, 1812.
- (13) (a) Baranoff, E.; Yum, J.-H.; Grätzel, M.; Nazeeruddin, M. K. *J. Organomet. Chem.* **2009**, *694*, 2661. (b) Schulz, G. L.; Holdcroft, S. *Chem. Mater.* **2008**, *20*, 5351. (c) Xu, Z.; Wu, Y.; Hu, B. *Appl. Phys. Lett.* **2006**, *89*, No. 131116. (d) Minaev, B. F.; Minaeva, V. A.; Baryshnikov, G. V.; Girtu, M. A.; Agren, H. *Russ. J. Appl. Chem.* **2009**, *82*, 1211.
- (14) (a) Jain, P. K.; Huang, X.; El-Sayed, I. H.; El-Sayed, M. A. *Acc. Chem. Res.* **2008**, *41*, 1578. (b) Daniel, M.-C.; Astruc, D. *Chem. Rev.* **2004**, *104*, 293. (c) Schmid, G.; Corain, B. *Eur. J. Inorg. Chem.* **2003**, 3081.
- (15) Gong, J. L.; Mullins, C. B. *Acc. Chem. Res.* **2009**, *42*, 1063.
- (16) (a) Lee, J. H.; Mahmoud, M. A.; Sitterle, V.; Sitterle, J.; Meredith, J. C. *J. Am. Chem. Soc.* **2009**, *131*, 5048. (b) Sakai, N.; Tatsumas, T. *Adv. Mater.* **2010**, *22*, 3185. (c) Wu, X. M.; Thrall, E. S.; Lu, H. T.; Steigerwald, M.; Brus, L. J. *Phys. Chem. C* **2010**, *114*, 12896.
- (17) (a) Moriggi, L.; Cannizzo, C.; Dumas, E.; Mayer, C. R.; Ulianov, A.; Helm, L. *J. Am. Chem. Soc.* **2009**, *131*, 10828. (b) Ojea-Jiménez, S.; Puentes, V. *J. Am. Chem. Soc.* **2009**, *131*, 13320.
- (18) (a) Mayer, C. R.; Dumas, E.; Miomandre, F.; Méallet-Renault, R.; Warmont, F.; Vigneron, J.; Pansu, R.; Etcheberry, A.; Sécheresse, F. *New J. Chem.* **2006**, *30*, 1628. (b) Mayer, C. R.; Cucchiari, G.; Jullien, J.; Dumur, F.; Marrot, J.; Dumas, E.; Sécheresse, F. *Eur. J. Inorg. Chem.* **2008**, 3614. (c) Mayer, C. R.; Dumas, E.; Sécheresse, F. *J. Colloid Interface Sci.* **2008**, *328*, 452. (d) Mayer, C. R.; Dumas, E.; Sécheresse, F. *Chem. Commun.* **2005**, 345.
- (19) Sako, K.; Kusakabe, M.; Tatemitsu, H. *Mol. Cryst. Liq. Cryst.* **1996**, *285*, 101.
- (20) Rabaça, S.; Almeida, M. *Coord. Chem. Rev.* **2010**, *254*, 1493.
- (21) Baudron, S. A.; Hosseini, M. W. *Inorg. Chem.* **2006**, *45*, 5260.
- (22) Curtin, P. N.; Tinker, L. L.; Burgess, C. M.; Cline, E. D.; Bernhard, S. *Inorg. Chem.* **2009**, *48*, 10498.
- (23) Zhu, J.; Ganton, M. D.; Kerr, M. A.; Workentin, M. S. *J. Am. Chem. Soc.* **2007**, *129*, 4904.
- (24) (a) Liu, S.-J.; Zhao, Q.; Fan, Q.-L.; Huang, W. *Eur. J. Inorg. Chem.* **2008**, 2177. (b) Dragonetti, C.; Falciola, L.; Mussini, P.; Righetto, S.; Roberto, D.; Ugo, R.; Valore, A.; De Angelis, F.; Fantacci, S.; Sgamellotti, A.; Ramon, M.; Muccini, M. *Inorg. Chem.* **2007**, *46*, 8533.
- (25) Zhu, Q.-Y.; Lu, W.; Zhang, Y.; Bian, G.-Q.; Gu, J.; Lin, X.-M.; Dai, J. *Eur. J. Inorg. Chem.* **2008**, 230.
- (26) Ladouceur, S.; Fortin, D.; Zysman-Colman, E. *Inorg. Chem.* **2010**, *49*, 5625.
- (27) (a) Lafalet, F.; Welter, S.; Popovic, Z.; De Cola, L. *J. Mater. Chem.* **2005**, *15*, 2820. (b) Du, F.; Zhou, H.; Chen, L.; Zhang, B.; Yan, B. *Trends Anal. Chem.* **2009**, *28*, 88. (c) Zhao, N.; Wu, Y.-H.; Wen, H.-M.; Zhang, X.; Chen, Z.-N. *Organometallics* **2009**, *28*, 5603.
- (28) Pramod, P.; Sudeep, P. K.; Thomas, K. G.; Kamat, P. V. *J. Phys. Chem. B* **2006**, *110*, 20737.
- (29) (a) Huang, W.; Masuda, G.; Maeda, S.; Tanaka, H.; Hino, T.; Ogawa, T. *Inorg. Chem.* **2008**, *47*, 468. (b) Staniszewski, A.; Heuer, W. B.; Meyer, G. J. *Inorg. Chem.* **2008**, *47*, 7062. (c) Baranoff, E.; Yum, J.-H.; Grätzel, M.; Nazeeruddin, M. K. *J. Organomet. Chem.* **2009**, *694*, 2661. (d) Sakai, N.; Tatsuma, T. *Adv. Mater.* **2010**, *22*, 3185.